

---

# DISCOVERY OF MAXIMALLY CONSISTENT CAUSAL ORDERS WITH LARGE LANGUAGE MODELS

---

A PREPRINT

 **Federico Baldo**

Sorbonne Université, INSERM,  
Institut Pierre Louis d'Epidémiologie  
et de Santé Publique,  
F75012, Paris, France

 **Simon Ferreira**

Sorbonne Université, INSERM,  
Institut Pierre Louis d'Epidémiologie  
et de Santé Publique,  
F75012, Paris, France

 **Charles K. Assaad**

Sorbonne Université, INSERM,  
Institut Pierre Louis d'Epidémiologie  
et de Santé Publique,  
F75012, Paris, France

## ABSTRACT

Causal discovery is essential for understanding complex systems, as it aims to uncover causal relationships from observational data in the form of a causal directed acyclic graph (DAG). However, traditional methods often rely on strong, untestable assumptions, which makes them unreliable in real applications. Large Language Models (LLMs) present a promising alternative for extracting causal knowledge from text-based metadata, which consolidates domain expertise. However, LLMs are prone to unreliability and hallucinations, necessitating strategies that account for their limitations. One such strategy involves leveraging a consistency measure to evaluate reliability. Additionally, most text metadata does not clearly distinguish direct causal relationships from indirect ones, further complicating the discovery of a causal DAG. As a result, focusing on causal orderings, rather than causal DAGs, emerges as a more practical and robust approach. We propose a novel method to derive a class of acyclic tournaments (representing plausible causal orders) that maximizes a consistency score derived from an LLM. Our approach begins by computing pairwise consistency scores between variables, yielding a semi-complete directed graph that aggregates these scores. From this structure, we identify optimal acyclic tournaments, prioritizing those that maximize consistency across all configurations. We tested our method on both well-established benchmarks, as well as real-world datasets from epidemiology and public health. Our results demonstrate the effectiveness of our approach in recovering a class of causal orders.

**Keywords** Causal Discovery, Large Language Models, Causal Order

## 1 Introduction

Causal discovery is a critical task in numerous scientific disciplines, such as epidemiology, economics, and biology, as it enables researchers to uncover the underlying relationships between variables and better understand complex systems. Traditionally, discovering causal directed acyclic graphs (DAGs) from data has been a challenging endeavor, as existing algorithms often rely on strong, untestable assumptions Spirtes et al. (2001); Glymour et al. (2019); Peters et al. (2017); Assaad et al. (2022), such as causal sufficiency or faithfulness, which may not hold in real-world scenarios Ait-Bachir et al. (2023). With the recent rise in the popularity of Large Language Models (LLMs), many have suggested that these models could provide a novel avenue for causal discovery Long et al. (2023a,b); Darvari et al. (2024); Cohrs et al. (2024b); Vashishtha et al. (2023). Unlike traditional causal discovery methods, LLMs operate

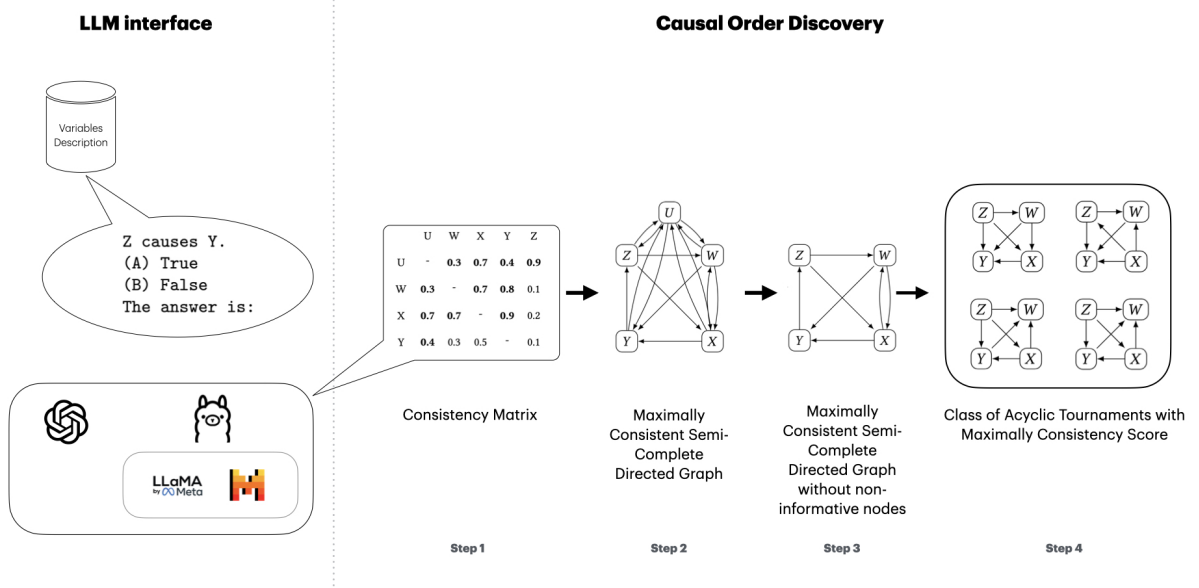


Figure 1: Pipeline of the LCOS algorithm. From the LLM we obtain the consistency matrix, then semi-complete directed graph maximizing the score. After the removal of uninformative edges, we extract the acyclic tournaments.

on textual data—leveraging pre-collected knowledge encoded in their training data Darvariu et al. (2024)—and may therefore require fewer assumptions to infer causal relationships.

However, despite growing interest, initial attempts to extract reliable causal information from LLMs have met limited success. In natural language, direct and indirect causes are often conflated, making them difficult to distinguish. This ambiguity is evident in various domains such as philosophy, biology, and epidemiology. For example, we often say that smoking causes cardiovascular disease, treating smoking as a direct cause. However, this relationship is most probably fully mediated by chronic inflammation and subclinical vascular pathology Al Rifai et al. (2017). Similarly, we commonly assert that a sedentary lifestyle causes type 2 diabetes, when in fact this link is fully mediated by obesity Li et al. (2022). More in general, in natural language, causal relations are frequently expressed as a simple relationship: “ $X$  causes  $Y$ ” or “ $X$  affects  $Y$ ” or “ $X$  prevents  $Y$ ”, etc. This oversimplification obscures the complex web of direct and indirect influences, including immediate “parents” and distant “ancestors” of a causal pathway. Given that LLMs are often characterized as “causal parrots” Zečević et al. (2023)—better suited for information retrieval than for inferring causal relationships—we argue that they are more effective for identifying causal orders rather than constructing detailed causal DAGs.

However, LLMs are notoriously unreliable, often producing hallucinated or inconsistent outputs. To mitigate this issue, we introduce, in this paper, the LLM-based Causal Order Search (LCOS) algorithm, which searches for a class of causal orders rather than identifying a single causal order. To achieve this, LCOS prompts the LLM in a pairwise manner, querying the causal relationship between each pair of variables while simultaneously quantifying the consistency or robustness of the responses. To this end, it computes a *consistency score* quantifying the degree of accordance of the LLM when queried multiple times with semantically equivalent questions. This strategy has proved effective in previous attempt at LLM driven causal discovery Long et al. (2023a); Darvariu et al. (2024); Cohrs et al. (2024b), and introduced in Kadavath et al. (2022). Subsequently, LCOS uses the scores to construct a maximally consistent semi-complete directed graph. It then uses an optimal method to discover a class of acyclic tournaments that are compatible with the semi-complete graph and represent a class of causal orders maximizing the heuristic. This approach ensures a more reliable extraction of causal information from LLMs despite their inherent limitations. Unlike traditional causal discovery methods Spirtes et al. (2001); Glymour et al. (2019); Peters et al. (2017); Assaad et al. (2022), our approach does not rely on classical assumptions, like causal sufficiency, faithfulness, or any other parametric assumptions. Instead, we assume only that the true causal graph is acyclic and that the LLM functions reasonably-well as an information retrieval tool.

**Contributions:**

- We provide an effective algorithm to discover a class of causal orders maximally consistent with the knowledge provided by LLMs. Such method is based on a top-down search strategy that does not require any parametric assumptions or causal sufficiency.
- We provide experimental evidence that our method can recover the causal orders with a high level of accuracy. We also provide reasonable realistic test cases that further prove the efficacy of our approach.

The remainder of the paper is organized as follows: in Section 2, we review relevant literature related to LLM-aided causal discovery; Section 4 represents the main contribution of the paper and describes in detail the proposed method; Section 5 presents the experimental results, followed by some discussion in Section ??; Section 6 concludes the paper and outlines future research directions.

## 2 Related Works

Causal discovery is an important challenge that scientists have addressed for many years. Indeed, many algorithms have been proposed to discover causal DAGs from observational data. Among these, we find constraint-based (Spirtes et al., 2001) (e.g., PC), noise-based (Shimizu et al., 2011; Peters et al., 2017) (e.g., LiNGAM), score-based (Chickering, 2003) (e.g., GES), and optimization-based (Zheng et al., 2018) (e.g., NOTEARS) families of algorithms Spirtes et al. (2001); Zheng et al. (2018). However, these methods often rely on strong, untestable assumptions that limit their practical applicability (Ait-Bachir et al., 2023). For instance, the PC algorithm Spirtes et al. (2001); Glymour et al. (2019), which relies on statistical conditional independence tests to identify independencies between variables, assumes faithfulness and causal sufficiency, i.e., no hidden confounding. Furthermore, some of these methods, including PC and GES, can only produce a class of graphs, known as Markov equivalent class (MEC) that contains all DAGs sharing the same conditional independencies as the true causal DAG. This class can be represented using a completed partially directed acyclic graph (CPDAG).

The recent rise of LLMs has opened a new avenue for causal discovery. New methods relying on LLMs as an oracle have been proposed to infer causal relationships. However, LLMs have been shown to be unreliable and untrustworthy; their tendency to produce hallucinations is a notable example of this issue. To tackle this problem while still leveraging the potential of LLMs in causal discovery, many researchers have suggested methods to quantify the reliability of these models. As presented in Cohrs et al. (2024a), there are two primary approaches to this task: the first is to compute the *uncertainty* of the LLM output using the probabilities associated to the tokens in the LLM’s response; the second is to evaluate the *consistency*, i.e., the coherence, of the LLM output when queried multiple times with semantically equivalent prompts.

In Cohrs et al. (2024b), authors propose an LLM informed variant of the PC algorithm. Specifically, the PC algorithm is enhanced by incorporating LLMs to detect conditional independencies among variables. The conditional independence is evaluated through the estimation of the  $p$ -value over the set of answers provided by the LLM to a set of equivalent queries; this approach closely resembles the consistency definition provided above. However, this method retains all the assumptions of the PC algorithm.

In Long et al. (2023a), a pairwise prompt strategy based on LLMs is used to complete the orientation of edges in a given CPDAG. Each edge is associated to an uncertainty —computed using the log probabilities associated to the response tokens—, then the MEC is refined through a Bayesian optimization process. In Darvari et al. (2024), the probabilities of pairwise causal relationship are computed using a strategy similar to Long et al. (2023a), and are provided to a causal discovery algorithm that incorporates them as priors, which are then used alongside observational data to find the causal DAG. Although not explicitly stated, these two approaches implicitly rely on the same assumptions as the chosen causal discovery algorithm.

The pairwise prompt strategy used in Long et al. (2023a); Darvari et al. (2024), requires a quadratic number of queries with respect to the number of variables. A more efficient approach to reduce the number of queries from quadratic to linear has been proposed in Jiralerspong et al. (2024). Starting from a set of variables deemed as prime causes, and provided explicitly by the LLM, the method learns the causal DAG through a BFS search. Specifically, the method expands the causal DAG by identifying new variables that are influenced by the visited nodes.

Concerning causal orders, Vashishtha et al. (2023) proposes a method for causal effect estimation through topological order and the application of the backdoor criterion Pearl (2009). More specifically, they rely on an LLM to provide a directed acyclic subgraph for each triplet of variables, which are then aggregated to obtain a causal order. Ties are resolved by using the LLM itself to make the final decision. This method identifies one order and does not directly address the unreliability of the LLM.

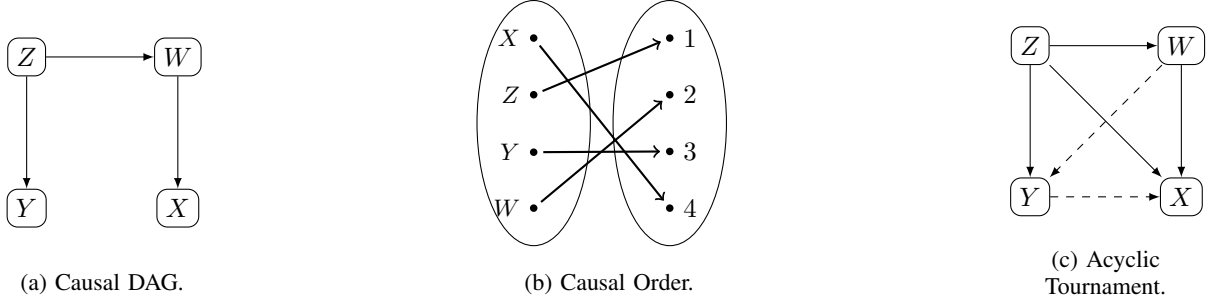


Figure 2: True graph and one of its possible causal orders and its corresponding acyclic tournament. Dashed lines represent edges that do not affect the topological order.

In this work, as in Vashishtha et al. (2023), we advocate that identifying causal orders rather than full causal DAGs presents a more intuitive task for LLMs, given the inherent causal ambiguity present in natural language. However, unlike Vashishtha et al. (2023), our approach focuses on discovering a causal order among variables by: (1) using a pairwise prompt strategy (2) leveraging consistency scores and (3) incorporating the uncertainty of the LLM by identifying a class of causal orders instead of a single causal order. Additionally, our method does not require observational data, thereby eliminating dependence on traditional causal discovery algorithms and their associated assumptions. Notably, our approach also does not assume causal sufficiency, making it more robust in scenarios where hidden confounding may be present.

### 3 Preliminaries

In this section, we introduce key concepts and notations related to causal inference.

A causal graph  $\mathcal{G} = (\mathbb{V}, \mathbb{E})$  consists of a set of nodes  $\mathbb{V}$  (or variables) and a set of directed edges  $\mathbb{E}$ . The existence of directed edge between two nodes indicates that there is a direct causal effect from  $X_i$  to  $X_j$ . Following standard causal assumptions Pearl (2009); Spirtes et al. (2001), we assume that  $\mathcal{G}$  is a directed acyclic graph (DAG), referred to as a *causal DAG*. In this paper, we assume that the causal DAG is unknown. Instead of attempting to reconstruct the DAG itself, we focus on discovering its corresponding causal order (Peters et al., 2017), defined as follows:

**Definition 1** (Causal Order). *Suppose a causal DAG  $\mathcal{G}$ . A causal order compatible with  $\mathcal{G}$  is a bijective mapping  $\pi : \mathbb{V} \mapsto \{1, \dots, d\}$  such that if  $Y$  is a descendant of  $X$  then  $\pi(X) < \pi(Y)$ ,  $\forall X, Y \in \mathbb{V}$ .*

It is important to note that, in general, multiple causal orders can be compatible with the same causal DAG. This occurs because a single DAG may permit several valid topological orderings of its nodes. Our approach seeks to identify a class of causal orders consistent with the underlying causal DAG. To represent a causal order graphically we utilize the concept of an acyclic tournament.

**Definition 2** (Acyclic tournament). *An acyclic tournament is a DAG with exactly one edge between each two vertices, in one of the two possible directions.*

An acyclic tournament provides a graphical representation that fully encodes a causal order. Specifically, the direction of the edge between any two nodes directly reflects their relative position in the causal order. An illustration of the relationship between a causal DAG, one of its corresponding causal orders, and the acyclic tournaments consistent with that order is presented in Figure 2.

In our paper, we will make use of an abstraction which will serve as an intermediary representation, capturing directed relationships between nodes without committing to a fully resolved causal order or acyclic structure. By searching for such an abstraction as a starting point, we can harness its structure to identify or constrain the set of compatible acyclic tournaments. The abstraction that will be used is a semi-complete directed graph defined as follows:

**Definition 3** (Semi-Complete Directed Graphs). *A directed graph is said to be semi-complete if there is at least one arc between each pair of its vertices.*

An illustration of different semi-complete directed graphs are presented in Figure 1 (Step 2) and (Step 3).

Notice that a semi-complete directed graph can contain cycles, which introduces significant complexity when analyzing these structures. To effectively work with such graphs throughout this paper, we rely on the concept of strongly connected components (SCCs).

**Definition 4** (Strongly connected components (SCCs)). *A strongly connected component is a subgraph of a directed graph in which each node is reachable from every other node.*

To establish a connection between semi-complete directed graphs and acyclic tournaments, we introduce the concept of compatibility, formalized in the following definition:

**Definition 5** (Compatible Acyclic Tournament). *Given a semi-complete directed graph  $S = (\mathbb{V}, \mathbb{E})$ , an acyclic tournament  $\mathcal{T}$  is said to be compatible with  $S$  if it can be derived from  $S$  by reversing certain edges within each SCC of  $S$ , while leaving all other edges unchanged.*

## 4 LLM-based Causal Order Search

This section presents the primary contribution of this paper: a novel algorithm, illustrated in Figure 1 and denoted as LCOS, for extracting causal knowledge from an LLM. The LCOS algorithm is specifically designed to discover causal orders among variables and its pseudo-code is given in Algorithm 1.

The LCOS algorithm adopts the pairwise prompt strategy introduced in Kıcıman et al. (2024); Long et al. (2023b)—Step 1, Figure 1—which involves asking the LLM to determine, for each pair of variables, which one is the cause (either direct or indirect) of the other, using detailed descriptions of both variables. However, as showed in Zečević et al. (2023), LLMs can be unreliable, as they are prone to hallucinations Huang et al. (2024). To address this issue, similarly to Kadavath et al. (2022), we compute a consistency score<sup>1</sup>, as defined in Cohrs et al. (2024a), which allows us to quantify the trustworthiness of the responses provided. The consistency score is computed by repeatedly querying the LLM with semantically equivalent prompt and evaluating the concordance of its responses on a causal relationship. This can help mitigate the unreliability of LLMs by prioritizing responses that are consistent across multiple iterations. Subsequently—Step 2, Figure 1—the LCOS algorithm constructs a semi-complete directed graph maximizing the consistency scores. To ensure that the graph reflects only meaningful causal relationships—Step 3, Figure 1—the LCOS algorithm eliminates uninformative variables, further refining the structure. Steps 1,2,3 of the LCOS algorithm are detailed in Section 4.1. Nevertheless, the graph obtained may not necessarily represent a valid causal order, as it could contain cycles or bidirected edges. To address this issue the LCOS algorithm employs an optimal search algorithm (Algorithm 2) designed to leverage the structure of semi-complete directed graphs—Step 4, Figure 1. This algorithm identifies the class of all possible acyclic tournaments that maximize the consistency scores among all possible acyclic tournaments. Further details of Step 4 of the LCOS algorithm are presented in Section 4.2.

### 4.1 Maximally Consistent Semi-Complete Directed Graphs

**Consistency Matrix** Following the approach adopted in Long et al. (2023a) and Kadavath et al. (2022), we assume to have a set of variables  $X_1, \dots, X_d$  with a set of descriptive metadata associated to each variable (i.e. a textual description of the variable),  $\mu_1, \dots, \mu_d$ . The queries are generated by prompting the LLM with a sentence of the form:

$\mu_i$  *verb* <sub>$k$</sub>   $\mu_j$ .  
 (A) True  
 (B) False  
 The answers is:

such that  $i \neq j$  and *verb* <sub>$k$</sub>  represents a causal verb, i.e. *verb* <sub>$k$</sub>   $\in$  {"cause", "provoke", "affect", ...}. We decided to rely on True/False questions based on the results obtained in Kadavath et al. (2022), which show that LLMs are generally well-calibrated for these types of prompts. Following Long et al. (2023a), we posed the same question  $n$  times with varying causal verbs, i.e.,  $\forall k, k' \in \{1, \dots, n\}$ , *verb* <sub>$k$</sub>   $\neq$  *verb* <sub>$k'$</sub> . This approach introduces slight perturbations to the input, allowing to evaluate the consistency of the LLM's responses under different phrasings. The proportion of True responses serves as our consistency score<sup>2</sup>. Specifically, when an LLM is queried  $n$  times about whether  $\mu_i$  causes  $\mu_j$ , and  $m$  of those responses are True, the consistency score for  $X_i \rightarrow X_j$  is calculated as:

$$C_{i \rightarrow j} = \frac{m}{n}.$$

<sup>1</sup>These scores, referred to as uncertainty scores in Kadavath et al. (2022), are renamed here to reflect their purpose more accurately: measuring the LLM's self-consistency when responding to the same causal question phrased in different ways.

<sup>2</sup>This notion of consistency reflects how consistent the LLM is in its answers which is different from the notion in Erdős and Moon (1965) where consistency reflects how close a tournament is from an ordering.

It is important to note that  $C_{i \rightarrow j}$  and  $C_{j \rightarrow i}$  are computed independently of each other. To facilitate computation and analysis, all consistency scores are precomputed and organized into a *consistency matrix*—Step 1, Figure 1—which stores the pairwise scores for each pair of variables.

**Maximally Consistent Semi-Complete Directed Graph** The consistency matrix is then used to build a maximally consistent semi-complete directed graph,  $\mathcal{S}$ . The graph  $\mathcal{S}$  is referred to as "maximally consistent" because it is constructed by analyzing the consistency matrix and selecting the directed edges between each pair of nodes based on the highest consistency score. Specifically, a directed edge  $X_i \rightarrow X_j$  is included in  $\mathcal{S}$  if  $C_{i \rightarrow j} \geq C_{j \rightarrow i}$ . Note that this implies that when  $C_{i \rightarrow j} = C_{j \rightarrow i}$  a bidirected edge would be formed between  $X_i$  and  $X_j$ . In Step 1 of Figure 1, the highest scores between each pair of variables are highlighted in the consistency matrix and are represented by an edge in the corresponding semi-complete directed graph Step 2, Figure 1.

**Non-Informative Nodes** It is important to note that some nodes in  $\mathcal{S}$ , might be connected to all other nodes exclusively through bidirected edges. In the graph shown in Step 2, Figure 1, we can observe that the vertex  $U$  is connected to every other node exclusively through bidirected edges. This implies that  $U$  can be placed in any position within the causal order based on the consistency score, making it non-informative. Interestingly, this holds true for any node defined as follows:

**Definition 6.** *Let  $\mathcal{S}$  be a maximally consistent semi-complete directed graph. We say that a vertex  $X$  in  $\mathcal{S}$  is non-informative if  $X$  has a bidirected edge with each other vertex in  $\mathcal{S}$ .*

Since these nodes are non-informative with respect to the causal order, we remove them from the graph. Retaining them would introduce unnecessary computational cost without adding value. In Step 3 of Figure 1, we remove the sole non-informative node  $U$ , resulting in a semi-complete directed graph deprived of non-informative nodes.

## 4.2 Maximally consistent Acyclic Tournaments

The maximally consistent semi-complete directed graph deprived of non-informative nodes,  $\mathcal{S}$ , obtained in Section 4.1 does not necessarily represent a valid causal order. Indeed, such a graph might include both cycles and bidirected edges. To obtain a class of plausible causal order, we need to find all maximally consistent acyclic tournaments that are compatible with the semi-complete directed graph.

**Definition 7** (Maximally consistent acyclic tournament (MCAT) compatible with  $\mathcal{S}$ ). *An acyclic tournament compatible with  $\mathcal{S}$  is said to be maximally consistent if it maximize the consistency score relative to all other acyclic tournaments compatible with  $\mathcal{S}$ .*

It is important to note that there might be many MCATs compatible with  $\mathcal{S}$ . To obtain them, we need to investigate all acyclic sub-tournaments compatible with each SCC in  $\mathcal{S}$ . Based on the SCCs, we might have different scenarios: on the one hand, we might have SCCs composed of single nodes (singletons), thus with a number of components equal to the number of nodes, implying that  $\mathcal{S}$  is already acyclic, i.e., there is only one acyclic MCAT compatible with  $\mathcal{S}$ . On the other hand, some SCCs may consist of multiple nodes. These components have to be transformed into maximally consistent acyclic sub-tournaments. This can be achieved by finding the minimal set of edges to reverse in the SCC in order to eliminate all cycles while maximizing the consistency score.

In the literature, the minimal set of edges that must be removed to transform an SCC into an acyclic subgraph is known as the Feedback Arc Set (FAS). A FAS is a smallest set of directed edges in the SCC that when removed eliminates all cycles from the SCC. However, since we are searching for a tournament rather than just any DAG, we require the resulting graph to remain fully connected. Fortunately, the FAS has a key property: instead of removing the selected edges, reversing all edges in the FAS also results in an acyclic graph, and in our case, an acyclic tournament Barthélemy et al. (1995). Moreover, in our context, we are not merely interested in any acyclicification of each SCC but rather in an acyclicification that maximizes the consistency score. Therefore, we focus on a weighted version of FAS, where the goal is to find a FAS that maximizes the sum of the weights associated to the edges. The most immediate solution would be to use the consistency scores of the edges as weights; however, given any pair of edges  $X_i \rightarrow X_j$  and  $X_k \rightarrow X_l$ , we generally have  $C_{i \rightarrow j} + C_{j \rightarrow i} \neq C_{k \rightarrow l} + C_{l \rightarrow k}$ . This implies that edges with lower consistency and capable of breaking the cycle are not necessarily a FAS. For example, suppose to have two edges  $X_i \rightarrow X_j$  and  $X_k \rightarrow X_l$  both capable of breaking a cycle in the SCC; let us also assume that  $C_{i \rightarrow j} = 0.6$  and its reverse  $C_{j \rightarrow i} = 0.1$ , while  $C_{k \rightarrow l} = 0.9$  and its reverse  $C_{l \rightarrow k} = 0.89$ . It is evident how reversing  $X_k \rightarrow X_l$  instead of  $X_i \rightarrow X_j$  results in a smaller decrease of the overall consistency. For this reason, we weight the edges in the graph with a *cost score*, defined as follows: let  $\xi$  be the total consistency score of  $\mathcal{S}$ , calculated as the sum of the consistency scores of all edges; for each edge  $X_i \rightarrow X_j$  in  $\mathcal{S}$ , the cost score  $B_{i \rightarrow j}$  is given by:

$$B_{i \rightarrow j} = \xi - C_{i \rightarrow j} + C_{j \rightarrow i}.$$

Reversing the edges of a FAS obtained with these weights —rather than removing them —gives an acyclic tournament which maximizes the overall consistency score.

To find a FAS from  $\mathcal{S}$  and the cost  $B$ , we use an exact solution, denoted as ExactFAS based on an integer programming formulation which is guaranteed to yield an optimal result. However, since, finding a FAS is NP-complete, ExactFAS can be too slow for very large SCCs. Nevertheless, assuming that the true causal graph is acyclic, we expect the SCCs to be relatively small, allowing for efficient detection of a FAS.

However, solving the FAS problem does not guarantee to find all the MCATs compatible with  $\mathcal{S}$ . Indeed, there might be multiple MCATs compatible with  $\mathcal{S}$ . This arises in presence of multiple FAS for the same SCC. Therefore, we propose a procedure, denoted as MCATsSearch and explicitly shown in Algorithm 2, to obtain all the MCATs compatible with  $\mathcal{S}$  by constraining the solution space based on previous solution of ExactFAS. More specifically, let  $\mathcal{T}$  be the first MCAT obtained by ExactFAS. Another MCAT  $\mathcal{T}'$  can be obtained by reversing a set of arcs,  $\mathbb{A}$ , which is not contained in the first optimal solution of ExactFAS,  $\mathbb{A}^*$  (line 3 of Algorithm 2). This means that  $\mathbb{A}$  is an optimal solution such that  $\mathbb{A} \neq \mathbb{A}^*$ . This is achieved by re-executing ExactFAS excluding from the admissible edges every subset  $\mathbb{F}$  of  $\mathbb{A}^*$ , i.e.,  $\mathbb{F} \in \mathcal{P}(\mathbb{A}^*)$ , as shown in line 11 of Algorithm 2. If the exclusion of  $\mathbb{F}$  leads to a suboptimal solution, i.e., of non-maximal score, then we exclude from the search all the subsets containing  $\mathbb{F}$ , such that  $\mathbb{F} \subset \mathbb{F}'$ , since they all lead to suboptimal solutions (line 21-23, Algorithm 2). The process is repeated for every optimal solution of the ExactFAS (line 17-19, Algorithm 2).

---

**Algorithm 1** LLM-based Causal Order Search (LCOS)
 

---

```

1: procedure LCOS( $\mathbb{V}$ : set of variables,  $D$ : descriptions of the variables)
2:    $C \leftarrow \text{LLMpairWiseConsistencyScores}(\mathbb{V}, D)$ 
3:    $(\mathbb{V}, \mathbb{E}) \leftarrow \text{maxConsSemiCompleteDG}(C)$ 
4:    $NI \leftarrow \text{nonInformativeNodes}(\mathbb{V}, \mathbb{E})$ 
5:    $(\mathbb{V}, \mathbb{E}) \leftarrow \text{removeVertices}(\mathbb{V}, \mathbb{E}, NI)$ 
6:    $\mathbb{S} \leftarrow \text{stronglyConnectedComponents}(\mathbb{V}, \mathbb{E})$ 
7:    $Solutions \leftarrow \emptyset$ 
8:   for  $\mathbb{V}_{SCC} \in \mathbb{S}$  do
9:     if  $|\mathbb{V}_{SCC}| > 1$  then
10:       $FAS_{SCC} \leftarrow \text{MCATsSearch}(\mathbb{V}_{SCC}, C)$ 
11:       $Solutions \leftarrow Solutions \times FAS_{SCC}$  ▷ combine different solution for different SCCs
12:    $res \leftarrow \emptyset$ 
13:   for  $\mathbb{E}_{FAS} \in Solutions$  do
14:      $res \leftarrow res \cup \text{Reverse}(\mathbb{V}, \mathbb{E}, \mathbb{E}_{FAS})$ 
return  $res$ 

```

---

The LCOS algorithm outputs all MCATs that are compatible with the semi-complete directed graph  $\mathcal{S}$  —Step 4, Figure 1. Interestingly, these tournaments are not only consistent with  $\mathcal{S}$  but also achieve the highest possible consistency score among all acyclic tournaments, whether they are compatible with  $\mathcal{S}$  or not. This result is formalized in the following proposition.

**Proposition 1.** *Suppose  $\mathcal{T}$  is an acyclic tournament of maximal consistence compatible with a maximally consistent semi-complete directed graph  $\mathcal{S}$ . It follows that  $\mathcal{T}$  is a maximally consistent acyclic tournament among all possible acyclic tournaments (compatible or not compatible with  $\mathcal{S}$ ).*

*Proof.* In Appendix B. □

**Practical Considerations** To reduce computational time, bidirected edges are handled separately. Before applying Algorithm 2, all bidirected edges are removed from the graph  $\mathcal{S}$ . After generating a class of acyclic tournaments, each bidirected edge is reintroduced as a directed edge, oriented in one of its possible directions. This is done ensuring that the new directed edge does not introduce new cycles. Since bidirected edges contribute equally to consistency, their orientation does not change the consistency score of the maximal acyclic tournament, but reduces the size of the SCCs that need to be transformed into acyclic sub-tournaments.

## 5 Experiments

The code was implemented in python 3.10. We relied on multiple LLMs as the backend for the LCOS algorithm. More specifically, all results presented in the paper were obtained using gpt-4o-mini for all the text-driven causal

**Algorithm 2** Maximally consistent acyclic tournaments search

---

```

1: procedure MCATsSEARCH( $\mathbb{V}$ : nodes,  $\mathbb{E}$ : edges,  $C$ : consistency matrix)
2:    $B \leftarrow \text{costScores}(\mathbb{V}, \mathbb{E}, C)$ 
3:    $\mathbb{A}^* \leftarrow \text{ExactFAS}(\mathbb{E}, B)$ 
4:    $Q \leftarrow \mathcal{P}(\mathbb{A}^*)$  ▷ queue of subsets
5:    $\mathbb{E}^* \leftarrow \text{Reverse}(\mathbb{V}, \mathbb{E}, \mathbb{A}^*)$ 
6:    $\text{maxCons} \leftarrow \text{consistency}(\mathbb{E}^*, C)$ 
7:    $\text{res} \leftarrow \{\mathbb{A}^*\}$ 
8:    $\text{mem} \leftarrow \emptyset$  ▷ cache for explored subsets
9:   while  $\neg Q.\text{empty}()$  do
10:     $F \leftarrow Q.\text{pop}()$ 
11:     $C' \leftarrow \text{modify}(\text{copy} = C, \text{index} = F, \text{value} = -\infty)$  ▷ sets to infinity the weights of the edges in  $F$ .
    Excludes edge in  $F$  from the admissible results.
12:     $\mathbb{A} \leftarrow \text{ExactFAS}(F, C')$ 
13:     $\mathbb{E}' \leftarrow \text{Reverse}(\mathbb{E}, \mathbb{A})$ 
14:     $\text{cons} \leftarrow \text{consistency}(\mathbb{E}', C')$ 
15:    if  $\text{cons} = \text{maxCons} \wedge \mathbb{A} \notin \text{res}$  then
16:       $\text{res} \leftarrow \text{res} \cup \{\mathbb{A}\}$ 
17:      for  $F' \in \mathcal{P}(A)$  do
18:        if  $F' \notin \text{mem} \wedge F' \notin Q$  then
19:           $Q.\text{push}(F')$ 
20:        else if  $\text{cons} < \text{maxCons}$  then
21:          for  $F' \in Q$  do
22:            if  $F \subset F'$  then
23:               $Q.\text{remove}(F')$ 
24:             $\text{mem} \leftarrow \text{mem} \cup \{F'\}$ 
return  $\text{res}$ 

```

---

discovery methods. This choice was made to facilitate comparison with other methods, which were implemented to work with `gpt-4o-mini`. However, we emphasize that our method was designed to be compatible with open-source LLMs, particularly those available through the `ollama` platform—a library that facilitates the management of multiple open-source LLMs. Among these we tested our method for: `llama3.1` with 8 billion parameters, and `mistral` with 7 billion parameters. All results obtained using `llama3.1` and `mistral` are available in Appendix D. For the implementation of graphs, we used `igraph`, a C++ library that offers an implementation of ExactFAS.

**Datasets** The LCOS algorithm, as well as all the other baselines, were tested on a total of 14 causal graphs with a minimum of 3 nodes and a maximum of 25 nodes, further details are provided in Appendix C. Among these, 4 are well-known causal DAGs included in the `bnlearn` library, namely Asia Lauritzen and Spiegelhalter (2018), Cancer Korb and Nicholson (2004), Child Spiegelhalter et al. (1993), and Sachs Sachs et al. (2005). Additionally, we utilized 10 real-world causal graphs, primarily sourced from the fields of epidemiology and public health. The corresponding ground truth causal DAGs were obtained from scientific literature. These causal DAGs include Covid 1, Covid 2, Covid 3 Griffith et al. (2020), Covid 4 Glemain et al. (2024) Genetic Palmer et al. (2012), MSU Piccininni et al. (2023), Neighborhood Chaix et al. (2009), Opioids Inoue et al. (2022), Climate Guevara et al. (2024), Supermarket Chaix et al. (2012). Notably, two of the selected graphs, MSU and Covid 1, do not satisfy causal sufficiency. For illustration, Figure ?? presents the MSU graph. Using realistic benchmarks—those that have not been extensively tested in the field of causal discovery—serves two purposes: first, they allow us to assess the effectiveness of our method in real-world scenarios; second, we aimed to evaluate any potential bias toward the `bnlearn` library, as it is widely used as a benchmark in causal discovery Long et al. (2023a); Darvari et al. (2024).

**Comparison with other methods** We compared the LCOS algorithm with state-of-the-art methods for LLM-aided causal discovery. Specifically, we focused on the methods introduced by (Long et al., 2023a), referred to as IE-LLM, and Jiralerspong et al. (2024), called BFS-LLM, as detailed in Section 2. Both of these methods were implemented using publicly available code<sup>3</sup><sup>4</sup>. Additionally, we considered a naive implementation of the PC algorithm presented in Cohrs et al. (2024b), which utilizes LLM for independence testing. We also implemented a version of the method

<sup>3</sup><https://github.com/StephLong614/Causal-disco-LLM-imperfect-experts>

<sup>4</sup><https://github.com/superkaiba/causal-llm-bfs>



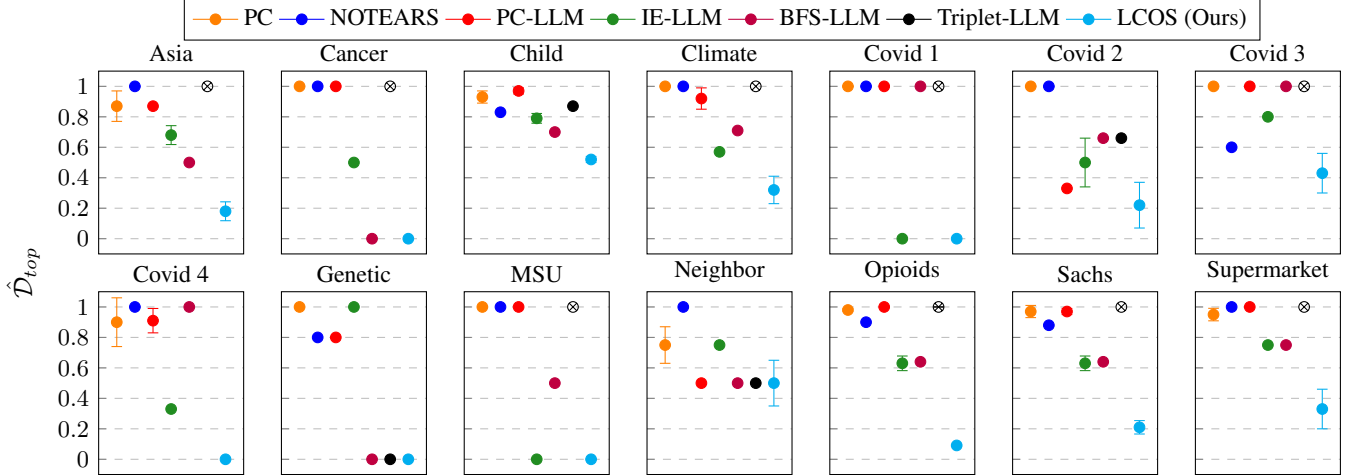


Figure 3: Mean and standard error of  $\hat{D}_{top}$  across all graphs in the class obtained by each method (the lower the better). Inconclusive experiments; i.e., results containing cycles or non terminating experiments, are regarded as having a maximum error, and are marked accordingly with  $\otimes$ .

presented in Vashishtha et al. (2023), which we refer to as Triplet-LLM<sup>5</sup>. To provide comprehensive overview of the LCOS algorithm’s potential, we tested the performance of conventional causal discovery approaches. Specifically, we conducted experiments using the PC algorithm with the KCI conditional independence test<sup>6</sup>, and a nonlinear version of NOTEARS<sup>7</sup>. Each data-driven method was tested on synthetic data generated from the true causal DAG following this formulation: for each node  $x$  in the DAG,

$$x = f_x(\text{Parents}(x)) + \epsilon_x,$$

where  $\text{Parents}(x)$  is the set of parents of  $x$  in the graph,  $f_x$  is a non-linear function, picked randomly from  $\{\sin(\cdot), \cos(\cdot), \text{square}(\cdot)\}$ , and  $\epsilon_x$  is sampled from a Gaussian distribution. We want to emphasize that we used non-linear functions to generate the data, but most of the data-driven algorithms tend to perform better when linearity holds. Indeed, we have created a hard experimental condition for conventional discovery methods. However, this choice is based on two considerations: first, non-linear relationships are prevalent in real-world data, and second, we aim to highlight the effectiveness of text-driven algorithms, which are not constrained by observational data and their parametric assumptions. Nevertheless, to provide a more complete overview of the results associated with the data-driven methods, we also report the results obtained by data-driven algorithms on linear synthetic data in Appendix D.

**Evaluation** The classical metrics used to estimate the error on the estimated causal graph are not as effective for evaluating the error on discovered causal orders. Indeed, there can be multiple causal orders that are consistent with the same causal DAG. To this end, we rely on a metric that closely resembles the one suggested in Ruiz et al. (2022); Rolland et al. (2022), that measures the error on the approximated causal order as the proportion of parents sorted after children concerning the true DAG,  $\mathcal{G}$ . Thus, for each node  $Y \in \mathcal{V}$ , a correct causal order assumes that for all parents of  $Y$ ,  $X \in \text{Parent}(Y)$ ,  $\pi(X) < \pi(Y)$ . The metric is then defined as follows:

$$\hat{D}_{top} = \frac{1}{|\mathbb{E}|} \sum_{u \in \mathcal{V}} \sum_{v \in \text{Desc}_{\hat{\mathcal{G}}}(u)} \mathbf{1}(v \notin \text{Desc}_{\mathcal{G}}(u))$$

where  $\mathcal{G}$  is the true causal DAG and  $\hat{\mathcal{G}}$  is the estimated DAG (for our method, the DAG is an acyclic tournament), and  $\mathbb{E}$  is the set of edges in  $\mathcal{G}$ . The metric  $\hat{D}_{top}$  is a normalized version of the metric proposed in Rolland et al. (2022).

Our method, along with some baseline methods, generates a class of graphs rather than a single graph. In such cases, we compute the  $\hat{D}_{top}$  metric for each graph within the class and report both the average and standard error across all graphs in the class. Furthermore, since our method does not include non-informative nodes in its final output,

<sup>5</sup>Our implementation is based on our understanding of the method presented in the paper. After being unable to find any publicly available code, we attempted to contact the authors, but received no response.

<sup>6</sup><https://github.com/py-why/causal-learn>

<sup>7</sup><https://github.com/xunzheng/notears>

we exclude these nodes from both the true causal DAG and the estimated DAG estimated by each method during evaluation.

**Results** Figure 3 presents the results from all baseline methods and the LCOS algorithm. As one can see, the LCOS algorithm consistently outperforms all others, except for the Neighborhood, MSU, Genetic, and Covid 2 graphs, where its performance matches that of one or two text-based methods, namely Triplet-LLM, IE-LLM, or BFS-LLM. More interestingly, LCOS successfully recovered a class of size 1 containing a true causal order in four cases, including two cases where hidden confounding was present (i.e., causal sufficiency was not satisfied), among these the causal DAG in Figure ?? . Additionally, for the largest graph considered, Opioids, containing 25 nodes, LCOS was able to retrieve a two causal orders with minimal error, significantly outperforming other methods. Based on the results, we do not observe a significant difference in the performance of LCOS between the graphs obtained from bnlearn and those derived from the epidemiology literature.

Regarding other text-driven methods, Triplet-LLM frequently yielded cyclic solutions, thereby violating our initial assumptions; in such cases, we regard the result as having a maximum error, specifically 1, and them marked accordingly ( $\otimes$ ). The same mark has been used in Figure 3 for inconclusive experiments —we were not able to run the Triplet-LLM method on the Opioids dataset. In contrast, BFS-LLM and IE-LLM successfully recover the true causal graph in some cases, namely, 2 times. Ultimately, the PC-LLM method was the weakest among the text-driven approaches.

Finally, data-driven methods tend to perform poorly. This is most probably due to the non-linear nature of the data. More detailed results are also documented in tabular format in Appendix D.

## 6 Conclusion

This paper presents a method for leveraging LLMs for causal discovery. Specifically, we focus on identifying a class of causal orders compatible with the knowledge provided by the LLM. Given that such knowledge can often be unreliable, our method aims to assess the consistency of the LLM before incorporating it into the discovery process. Our approach is based on a top-down search strategy that does not require any parametric assumptions or causal sufficiency. We provide extensive experimental evidence demonstrating that our method can accurately recover a set of causal orders, which frequently includes at least one correct order from the true causal order. Furthermore, we compare our method with other approaches for causal discovery based on LLMs, and we show that our method outperforms them. We also present realistic test cases that further validate the efficacy of our approach, including real-world datasets extracted from public health and epidemiology literature.

The main limitation of this work, and any other LLM-based method, is that it relies on the assumption that the LLM provides reasonably accurate information about causal relationships through consistency scores. While our intuition appears to hold in practice, we cannot guarantee that this is always the case.

We have identified key areas for improving and extending of our method, namely: 1) testing our approach using a chain-of-thought based LLMs, 2) developing an optimal strategy for finding the best description of the variables, 3) reducing computational complexity, and 4) providing causal inference methodologies based on classes of acyclic tournaments such that at least one of them represent a valid causal order.

## Acknowledgments

This work was supported by the CIPHOD project (ANR-23-CPJ1-0212-01).

## References

- Mahmoud Al Rifai, Andrew P. DeFilippis, John W. McEvoy, Michael E. Hall, Ana Navas Acien, Miranda R. Jones, Rachel Keith, Hoda S. Magid, Carlos J. Rodriguez, Graham R. Barr, Emelia J. Benjamin, Rose Marie Robertson, Aruni Bhatnagar, and Michael J. Blaha. 2017. The relationship between smoking intensity and subclinical cardiovascular injury: The Multi-Ethnic Study of Atherosclerosis (MESA). *Atherosclerosis* 258 (2017), 119–130. <https://doi.org/10.1016/j.atherosclerosis.2017.01.021>
- Charles K. Assaad, Emilie Devijver, and Eric Gaussier. 2022. Survey and Evaluation of Causal Discovery Methods for Time Series. 73 (5 May 2022). <https://doi.org/10.1613/jair.1.13428>
- Ali Ait-Bachir, Charles K. Assaad, Christophe de Bignicourt, Emilie Devijver, Simon Ferreira, Eric Gaussier, Hosein Mohanna, and Lei Zan. 2023. Case Studies of Causal Discovery from IT Monitoring Time Series.

- arXiv:2307.15678 [cs.LG] The History and Development of Search Methods for Causal Structure Workshop at the 39th Conference on Uncertainty in Artificial Intelligence.
- Jean-Pierre Barthélemy, Olivier Hudry, Garth Isaak, Fred S. Roberts, and Barry Tesman. 1995. The reversing number of a diagraph. *Discrete Applied Mathematics* 60, 1 (1995), 39–76. [https://doi.org/10.1016/0166-218X\(94\)00042-C](https://doi.org/10.1016/0166-218X(94)00042-C)
- Basile Chaix, Kathy Bean, Mark Daniel, Shannon Zenk, Yan Kestens, H el ene Charreire, Cinira Leal, Fr ed erique Thomas, No ella Karusisi, Christiane Weber, Jean-Michel Oppert, Chantal Simon, Juan Merlo, and Bruce Pannier. 2012. Associations of Supermarket Characteristics with Weight Status and Body Fat: A Multilevel Analysis of Individuals within Supermarkets (RECORD Study). *PLoS one* 7 (04 2012), e32908. <https://doi.org/10.1371/journal.pone.0032908>
- Basile Chaix, Cinira Leal, and David Evans. 2009. Neighborhood-level Confounding in Epidemiologic Studies Unavoidable Challenges, Uncertain Solutions. *Epidemiology (Cambridge, Mass.)* 21 (11 2009), 124–7. <https://doi.org/10.1097/EDE.0b013e3181c04e70>
- David Maxwell Chickering. 2003. Optimal structure identification with greedy search. *J. Mach. Learn. Res.* 3, null (March 2003), 507–554. <https://doi.org/10.1162/153244303321897717>
- Kai-Hendrik Cohrs, Emiliano Diaz, Vasileios Sitokonstantinou, Gherardo Varando, and Gustau Camps-Valls. 2024a. Large Language Models for Causal Hypothesis Generation in Science. *Machine Learning: Science and Technology* (2024).
- Kai-Hendrik Cohrs, Gherardo Varando, Emiliano Diaz, Vasileios Sitokonstantinou, and Gustau Camps-Valls. 2024b. Large Language Models for Constrained-Based Causal Discovery. arXiv:2406.07378 [cs.AI] <https://arxiv.org/abs/2406.07378>
- Victor-Alexandru Darvari, Stephen Hailes, and Mirco Musolesi. 2024. Large Language Models are Effective Priors for Causal Graph Discovery. *arXiv preprint arXiv:2405.13551* (2024).
- P. Erdős and J. W. Moon. 1965. On Sets of Consistent Arcs in a Tournament. *Canad. Math. Bull.* 8, 3 (1965), 269–271. <https://doi.org/10.4153/CMB-1965-017-1>
- Benjamin Glemain, Charles Assaad, Walid Ghosn, Paul Moulair, Xavier de Lamballerie, Marie Zins, Gianluca Severi, Mathilde Touvier, Jean-Fran ois Deleuze, SAPRIS-SERO study group, Nathana el Lapidus, and Fabrice Carrat. 2024. Does hospital overload increase the risk of death when infected by SARS-CoV-2? *medRxiv* (2024). <https://doi.org/10.1101/2024.08.26.24312569>
- Clark Glymour, Kun Zhang, and Peter Spirtes. 2019. Review of Causal Discovery Methods Based on Graphical Models. *Frontiers in Genetics* 10 (2019). <https://doi.org/10.3389/fgene.2019.00524>
- Gareth J. Griffith, Tim T. Morris, Matthew J Tudball, Annie Herbert, Giulia Mancano, Lindsey Pike, Gemma C. Sharp, Jonathan A. C. Sterne, Tom M. Palmer, George Davey Smith, Kate Tilling, Luisa Zuccolo, Neil Martin Davies, and Gibran Hemani. 2020. Collider bias undermines our understanding of COVID-19 disease risk and severity. *Nature Communications* 11 (2020). <https://api.semanticscholar.org/CorpusID:218937284>
- Laura Andrea Barrero Guevara, Sarah C Kramer, Tobias Kurth, and Matthieu Domenech de Cell es. 2024. Causal inference concepts can guide research into the effects of climate on infectious diseases. (2024). arXiv:2402.12507 [q-bio.PE] <https://arxiv.org/abs/2402.12507>
- Lei Huang, Weijiang Yu, Weitao Ma, Weihong Zhong, Zhangyin Feng, Haotian Wang, Qianglong Chen, Weihua Peng, Xiaocheng Feng, Bing Qin, and Ting Liu. 2024. A Survey on Hallucination in Large Language Models: Principles, Taxonomy, Challenges, and Open Questions. *ACM Transactions on Information Systems* (Nov. 2024). <https://doi.org/10.1145/3703155>
- Kosuke Inoue, Beate Ritz, and Onyebuchi A Arah. 2022. Causal Effect of Chronic Pain on Mortality Through Opioid Prescriptions: Application of the Front-Door Formula. *Epidemiology* 33, 4 (2022), 572–580.
- Thomas Jiralerspong, Xiaoyin Chen, Yash More, Vedant Shah, and Yoshua Bengio. 2024. Efficient causal graph discovery using large language models. *arXiv preprint arXiv:2402.01207* (2024).
- Saurav Kadavath, Tom Conerly, Amanda Askell, Tom Henighan, Dawn Drain, Ethan Perez, Nicholas Schiefer, Zac Hatfield-Dodds, Nova DasSarma, Eli Tran-Johnson, Scott Johnston, Sheer El-Showk, Andy Jones, Nelson Elhage, Tristan Hume, Anna Chen, Yuntao Bai, Sam Bowman, Stanislav Fort, Deep Ganguli, Danny Hernandez, Josh Jacobson, Jackson Kernion, Shauna Kravec, Liane Lovitt, Kamal Ndousse, Catherine Olsson, Sam Ringer, Dario Amodei, Tom Brown, Jack Clark, Nicholas Joseph, Ben Mann, Sam McCandlish, Chris Olah, and Jared Kaplan. 2022. Language Models (Mostly) Know What They Know. arXiv:2207.05221 [cs.CL] <https://arxiv.org/abs/2207.05221>

- Kevin B. Korb and Ann E. Nicholson. 2004. Bayesian Artificial Intelligence. (2004). <https://api.semanticscholar.org/CorpusID:203667732>
- Emre Kıcıman, Robert Ness, Amit Sharma, and Chenhao Tan. 2024. Causal Reasoning and Large Language Models: Opening a New Frontier for Causality. (2024). arXiv:2305.00050 [cs.AI] <https://arxiv.org/abs/2305.00050>
- S. L. Lauritzen and D. J. Spiegelhalter. 2018. Local Computations with Probabilities on Graphical Structures and Their Application to Expert Systems. *Journal of the Royal Statistical Society: Series B (Methodological)* 50, 2 (12 2018), 157–194. <https://doi.org/10.1111/j.2517-6161.1988.tb01721.x> arXiv:[https://academic.oup.com/jrsssb/article-pdf/50/2/157/49097926/jrsssb\\_50\\_2\\_157.pdf](https://academic.oup.com/jrsssb/article-pdf/50/2/157/49097926/jrsssb_50_2_157.pdf)
- Dan-dan Li, Yang Yang, Zi-yi Gao, Li-hua Zhao, Xue Yang, Feng Xu, Chao Yu, Xiu-lin Zhang, Xue-Qin Wang, Li-hua Wang, and Jian-Bin Su. 2022. Sedentary lifestyle and body composition in type 2 diabetes. *Diabetology & Metabolic Syndrome* 14 (01 2022). <https://doi.org/10.1186/s13098-021-00778-6>
- Stephanie Long, Alexandre Piché, Valentina Zantedeschi, Tibor Schuster, and Alexandre Drouin. 2023a. Causal Discovery with Language Models as Imperfect Experts. arXiv:2307.02390 [cs.AI] <https://arxiv.org/abs/2307.02390>
- Stephanie Long, Tibor Schuster, and Alexandre Piché. 2023b. Can large language models build causal graphs? *arXiv preprint arXiv:2303.05279* (2023).
- Tom M. Palmer, Deborah A. Lawlor, Roger M. Harbord, Nuala A. Sheehan, Jonathan H. Tobias, Nicholas John Timpson, George Davey Smith, and Jonathan A. C. Sterne. 2012. Using multiple genetic variants as instrumental variables for modifiable risk factors. *Statistical Methods in Medical Research* 21 (2012), 223 – 242. <https://api.semanticscholar.org/CorpusID:14863122>
- Judea Pearl. 2009. *Causality: Models, Reasoning and Inference* (2 ed.). Cambridge University Press, Cambridge. <https://doi.org/10.1017/CB09780511803161>
- Jonas Peters, Dominik Janzing, and Bernhard Schölkopf. 2017. *Elements of Causal Inference: Foundations and Learning Algorithms*. The MIT Press.
- Marco Piccininni, Tobias Kurth, Heinrich J Audebert, and Jessica L Rohmann. 2023. The effect of mobile stroke unit care on functional outcomes: an application of the front-door formula. *Epidemiology* 34, 5 (2023), 712–720.
- Paul Rolland, Volkan Cevher, Matthäus Kleindessner, Chris Russel, Bernhard Schölkopf, Dominik Janzing, and Francesco Locatello. 2022. Score matching enables causal discovery of nonlinear additive noise models. (2022). arXiv:2203.04413 [cs.LG] <https://arxiv.org/abs/2203.04413>
- Gabriel Ruiz, Oscar Hernan Madrid Padilla, and Qing Zhou. 2022. Sequentially learning the topological ordering of causal directed acyclic graphs with likelihood ratio scores. (2022). arXiv:2202.01748 [stat.ME] <https://arxiv.org/abs/2202.01748>
- Karen Sachs, Omar D. Perez, Dana Pe’er, Douglas A. Lauffenburger, and Garry P. Nolan. 2005. Causal Protein-Signaling Networks Derived from Multiparameter Single-Cell Data. *Science* 308 (2005), 523 – 529. <https://api.semanticscholar.org/CorpusID:8160280>
- Shohei Shimizu, Takanori Inazumi, Yasuhiro Sogawa, Aapo Hyvärinen, Yoshinobu Kawahara, Takashi Washio, Patrik O. Hoyer, and Kenneth Bollen. 2011. DirectLiNGAM: A Direct Method for Learning a Linear Non-Gaussian Structural Equation Model. *J. Mach. Learn. Res.* 12, null (July 2011), 1225–1248.
- David J Spiegelhalter, A Philip Dawid, Steffen L Lauritzen, and Robert G Cowell. 1993. Bayesian analysis in expert systems. *Statistical science* (1993), 219–247.
- Peter Spirtes, Clark Glymour, and Richard Scheines. 2001. *Causation, prediction, and search*. MIT press.
- Aniket Vashishtha, Abbavaram Gowtham Reddy, Abhinav Kumar, Saketh Bachu, Vineeth N Balasubramanian, and Amit Sharma. 2023. Causal Inference Using LLM-Guided Discovery. arXiv:2310.15117 [cs.AI] <https://arxiv.org/abs/2310.15117>
- Matej Zečević, Moritz Willig, Devendra Singh Dhami, and Kristian Kersting. 2023. Causal Parrots: Large Language Models May Talk Causality But Are Not Causal. *Transactions on Machine Learning Research* (2023). <https://openreview.net/forum?id=tv46tCzs83>
- Xun Zheng, Bryon Aragam, Pradeep Ravikumar, and Eric P. Xing. 2018. DAGs with NO TEARS: continuous optimization for structure learning. In *Proceedings of the 32nd International Conference on Neural Information Processing Systems* (Montréal, Canada) (*NIPS’18*). Curran Associates Inc., Red Hook, NY, USA, 9492–9503.

## A Appendix

### B Proof of Proposition 1

To prove Proposition B, we need first to define the notion of Component Graphs.

**Definition 8** (Component Graph). *Let  $\mathcal{G} = (\mathbb{V}, \mathbb{E})$  be a directed graph. The components graph of  $\mathcal{G}$  is the graph  $\mathcal{G}_\sigma = (\mathbb{V}_\sigma, \mathbb{E}_\sigma)$  where  $\mathbb{V}_\sigma = \{\sigma_1, \sigma_2, \dots, \sigma_k\}$  is the set of strongly connected components of  $\mathcal{G}$  and  $\mathbb{E}_\sigma = \{(\sigma_i, \sigma_j) \mid \exists u \in \sigma_i, v \in \sigma_j \text{ such that } (u, v) \in \mathbb{E}\}$ .*

Definition 8 can be applied to abstract the strongly connected components of the maximally consistent semi-complete graph. In Figure 4, we present the components graph.

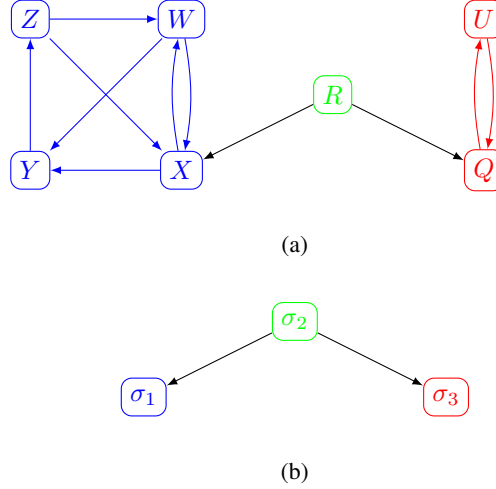


Figure 4: (a) Semicomplete graph; (b) Relative component graph.

Now we recall Proposition 1 and then we prove it.

**Proposition 1.** *Suppose  $\mathcal{T}$  is an acyclic tournament of maximal consistence compatible with a maximally consistent semi-complete directed graph  $\mathcal{S}$ . It follows that  $\mathcal{T}$  is a maximally consistent acyclic tournament among all possible acyclic tournaments (compatible or not compatible with  $\mathcal{S}$ ).*

*Proof.* Suppose we have the maximally consistent semi-complete graph  $\mathcal{S}$ . We define the components graph of  $\mathcal{S}$  as  $\mathcal{S}_\sigma = (\mathbb{V}_\sigma, \mathbb{E}_\sigma)$ . Let us assume that  $\mathcal{T}$  is an acyclic tournament of maximal consistence that is not compatible with  $\mathcal{S}$ . We can build a graph  $\mathcal{T}'$  compatible with  $\mathcal{S}$  orienting all the edges in  $\mathcal{T}$  according to  $\mathbb{E}_\sigma$ . The graph  $\mathcal{T}'$  can be either acyclic or cyclic:

- If  $\mathcal{T}'$  is acyclic, then  $\mathcal{T}$  can not be maximally consistent. Indeed, since  $\mathcal{S}$  is maximally consistent,  $\mathcal{T}'$  has higher consistency than  $\mathcal{T}$ , violating the initial assumption;
- If  $\mathcal{T}'$  is cyclic, it exists a cycle  $\mathbb{C} \in \mathcal{T}'$  and  $\mathbb{C} \notin \mathcal{T}$ , which implies that  $\mathbb{E}_\sigma \cap \mathbb{C} \neq \emptyset$ . Namely, there is a cycle that includes some of the edges in  $\mathbb{E}_\sigma$ . We can now construct new cycles  $\mathbb{C}'$  in  $\mathcal{S}$  that includes edges in  $\mathbb{E}_\sigma$  by replacing every edge  $(u, v) \in \mathbb{C} \setminus \mathbb{E}_\sigma$  with a directed path from  $u$  to  $v$  in  $\mathcal{S}$ . The direct path from  $u$  to  $v$  exists in  $\mathcal{S}$  since  $(u, v) \notin \mathbb{E}_\sigma$ , thus they must be part of strongly connected component. At this point,  $\mathbb{C}'$  is a cycle in  $\mathcal{S}$ , that contains edges in  $\mathbb{E}_\sigma$ , which contradicts the definition of  $\mathbb{E}_\sigma$ .

□

## C Graphs

The following table shows the specifics of each graph described in Section 5.

Dataset	Nodes	Edges
Asia Lauritzen and Spiegelhalter (2018)	8	8
Cancer Korb and Nicholson (2004)	5	4
Child Spiegelhalter et al. (1993)	20	27
Climate Guevara et al. (2024)	8	8
Covid 1 Griffith et al. (2020)	3	2
Covid 2 Griffith et al. (2020)	4	5
Covid 3 Griffith et al. (2020)	4	3
Covid 4 Glemain et al. (2024)	4	6
Genetic Palmer et al. (2012)	6	5
MSU Piccininni et al. (2023)	5	6
Neighborhood Chaix et al. (2009)	5	8
Opioids Inoue et al. (2022)	25	31
Sachs Sachs et al. (2005)	11	17
Supermarket Chaix et al. (2012)	7	12

Table 1: Datasets used in the experiments.

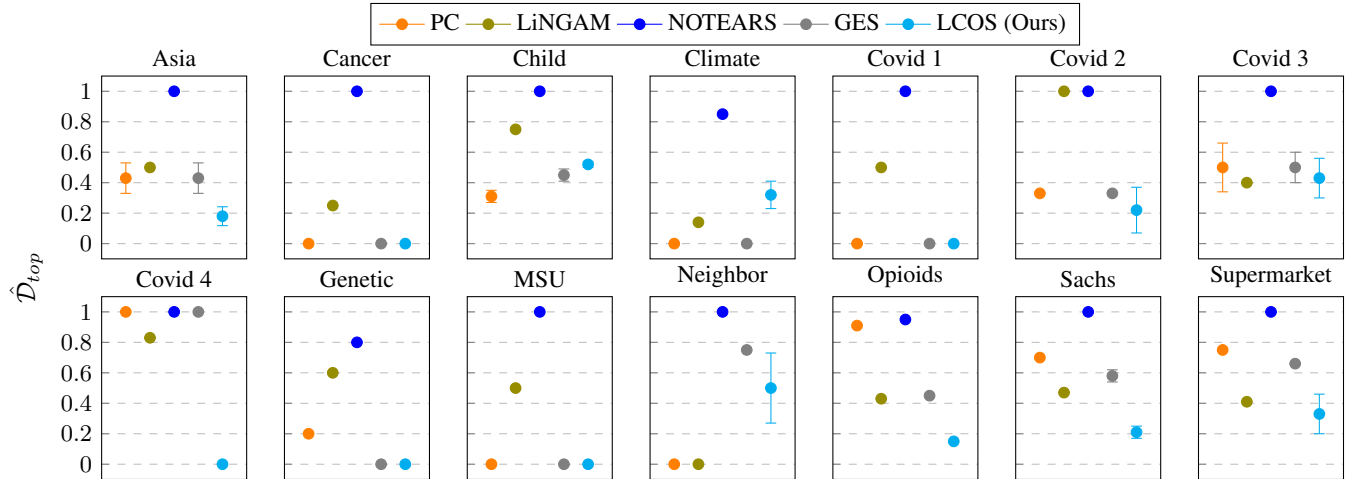


Figure 5: Mean and standard error of  $\hat{D}_{top}$  across all graphs in the class obtained by each method (the lower the better) for data-driven methods. Data are generated assuming linearity and gaussian noise. Inconclusive experiments; i.e., results containing cycles or non terminating experiments, are regarded as having a maximum error, and are marked accordingly with  $\otimes$ .

## D Additional Results

Following we provide additional results for the baselines presented in Section 5 and 2 and the LCOS algorithm presented in Section 4. Table 2 provides the main results concerning text-driven methods—including the LCOS algorithm—in tabular form. We underlying for each method that outputs a class of graphs the best results, mean and standard error across all graphs in the class, and the size of the class. Table 3 and Figure 5 show the results obtained on data-driven methods assuming linear causal relationships and gaussian noise; Table 4 and Figure 6, instead, show the results on the same method assuming linear causal relationships and uniform noise—we can clearly see how LiNGAM outperforms all other methods in this case. Ultimately, Table 5 provides the results of the LCOS algorithm using different LLMs as backend to build the consistency matrix.

Dataset	Top. Error	Text-Driven				
		PC-LLM	IE-LLM	BFS-LLM	Triplet-LLM	LCOS (Ours)
Asia	Best	0.87	0.62	0.5	⊗	0.12
	Avg	$0.87 \pm 0.0$	$0.68 \pm 0.062$	-	-	$0.18 \pm 0.062$
	Size	1	4	-	-	6
Cancer	Best	1.0	0.50	0.0	⊗	0.0
	Size	$0.87 \pm 0.0$	$0.68 \pm 0.062$	-	-	$0 \pm 0$
	Avg	1	1	-	-	1
Child	Best	0.95	0.75	0.70	0.87	0.41
	Avg	$0.97 \pm 0.02$	$0.79 \pm 0.032$	-	-	$0.52 \pm 0.020$
	Size	2	512	-	-	10
Climate	Best	0.85	0.57	0.71	⊗	0.14
	Avg	$0.92 \pm 0.07$	$0.57 \pm 0.0$	-	-	$0.32 \pm 0.09$
	Size	2	1	-	-	7
Covid 1	Best	1.0	0.0	1.0	⊗	0.0
	Avg	$1.0 \pm 0.0$	$0.0 \pm 0.0$	-	-	$0.0 \pm 0.0$
	Size	1	1	-	-	2
Covid 2	Best	0.33	0.3	0.66	0.66	0.0
	Avg	$0.33 \pm 0.0$	$0.5 \pm 0.16$	-	-	$0.22 \pm 0.15$
	Size	1	2	-	-	3
Covid 3	Best	1.0	0.8	1.0	⊗	0.2
	Avg	$1.0 \pm 0.0$	$0.8 \pm 0.0$	-	-	$0.43 \pm 0.13$
	Size	1	2	-	-	6
Covid 4	Best	0.83	0.33	1.0	⊗	0.0
	Avg	$0.91 \pm 0.08$	$0.33 \pm 0.0$	-	-	$0.0 \pm 0.0$
	Size	2	2	-	-	1
Genetic	Best	0.8	1.0	0.0	0.0	0.0
	Avg	$0.8 \pm 0.0$	$1.0 \pm 0.0$	-	-	$0.0 \pm 0.0$
	Size	1	1	-	-	4
MSU	Best	1.0	0.0	0.5	⊗	0.0
	Avg	$1.0 \pm 0.0$	$0.5 \pm 0.0$	-	-	$0.0 \pm 0.0$
	Size	4	1	-	-	1
Neighborhood	Best	0.5	0.75	0.5	0.5	0.16
	Avg	$0.5 \pm 0.0$	$0.75 \pm 0.0$	-	-	$0.5 \pm 0.15$
	Size	4	1	-	-	7
Opioids	Best	1.0	0.57	0.88	-	0.088
	Avg	$1.0 \pm 0.0$	$0.57 \pm 0.0$	-	-	$0.091 \pm 0.003$
	Size	1	2	-	-	2
Sachs	Best	0.94	0.58	0.64	⊗	0.11
	Avg	$0.97 \pm 0.02$	$0.63 \pm 0.048$	-	-	$0.21 \pm 0.044$
	Size	8	64	-	-	378
Supermark	Best	1.0	0.75	0.75	⊗	0.16
	Avg	$1.0 \pm 0.0$	$0.75 \pm 0.0$	-	-	$0.33 \pm 0.13$
	Size	1	4	-	-	24

Table 2: Best result, mean and standard error of  $\hat{\mathcal{D}}_{top}$  across all graphs in the class obtained by each method (the lower the better) for text-driven methods. The size of the class obtained is reported for each method. Inconclusive experiments; i.e., results containing cycles or non terminating experiments, are regarded as having a maximum error, and are marked accordingly with  $\otimes$ .

Dataset	Top. Error	Methods				
		PC	LiNGAM	NOTEARS	GES	LCOS (Ours)
Asia	Best	0.37	0.5	1.0	0.37	0.12
	Avg	$0.43 \pm 0.10$	-	-	$0.43 \pm 0.10$	$0.18 \pm 0.062$
	Size	2	-	-	2	6
Cancer	Best	0.0	0.25	1.0	0.0	0.0
	Avg	$0.0 \pm 0.0$	-	-	$0.0 \pm 0.0$	$0 \pm 0$
	Size	1	-	-	1	1
Child	Best	0.29	0.75	1.0	0.45	0.41
	Avg	$0.31 \pm 0.04$	-	-	$0.45 \pm 0.04$	$0.52 \pm 0.020$
	Size	8	-	-	8	10
Climate	Best	0.0	0.14	0.85	0.0	0.14
	Avg	$0.0 \pm 0.0$	-	-	$0.0 \pm 0.0$	$0.32 \pm 0.09$
	Size	1	-	-	1	7
Covid 1	Best	0.0	0.5	1.0	0.0	0.0
	Avg	$0.0 \pm 0.0$	-	-	$0.0 \pm 0.0$	$0.0 \pm 0.0$
	Size	1	-	-	1	2
Covid 2	Best	0.33	1.0	1.0	0.33	0.0
	Avg	$0.33 \pm 0.0$	-	-	$0.33 \pm 0.0$	$0.22 \pm 0.15$
	Size	2	-	-	2	3
Covid 3	Best	0.40	0.4	1.0	0.4	0.2
	Avg	$0.50 \pm 0.16$	-	-	$0.5 \pm 0.1$	$0.43 \pm 0.13$
	Size	2	-	-	2	6
Covid 4	Best	1.0	0.83	1.0	1.0	0.0
	Avg	$1.0 \pm 0.0$	-	-	$1.0 \pm 0.0$	$0.0 \pm 0.0$
	Size	2	-	-	4	1
Genetic	Best	0.20	0.6	0.8	0.0	0.0
	Avg	$0.20 \pm 0.0$	-	-	$0.0 \pm 0.0$	$0.0 \pm 0.0$
	Size	1	-	-	1	4
MSU	Best	0.0	0.5	1.0	0.0	0.0
	Avg	$0.0 \pm 0.0$	-	-	$0.0 \pm 0.0$	$0.0 \pm 0.0$
	Size	1	-	-	1	1
Neighborhood	Best	0.0	0.0	1.0	0.75	0.16
	Avg	$0.0 \pm 0.0$	-	-	$0.75 \pm 0.0$	$0.5 \pm 0.15$
	Size	4	-	-	8	7
Opioids	Best	0.90	0.43	0.95	0.45	0.088
	Avg	$0.91 \pm 0.01$	-	-	$0.45 \pm 0.0$	$0.091 \pm 0.003$
	Size	256	-	-	1	2
Sachs	Best	0.70	0.47	1.0	0.58	0.11
	Avg	$0.70 \pm 0.01$	-	-	$0.58 \pm 0.04$	$0.21 \pm 0.044$
	Size	1	-	-	1	378
Supermarket	Best	0.75	0.41	1.0	0.66	0.16
	Avg	$0.75 \pm 0.01$	-	-	$0.66 \pm 0.0$	$0.33 \pm 0.13$
	Size	1	-	-	8	24

Table 3: Best result, mean and standard error of  $\hat{\mathcal{D}}_{top}$  across all graphs in the class obtained by each method (the lower the better) for data-driven methods. The size of the class obtained is reported for each method. Data are generated assuming linearity and gaussian noise. Inconclusive experiments; i.e., results containing cycles or non terminating experiments, are regarded as having a maximum error, and are marked accordingly with  $\otimes$ .



Dataset	Top. Error	Methods				
		PC	LiNGAM	NOTEARS	GES	LCOS (Ours)
Asia	Best	0.37	0.0	1.0	0.0	0.12
	Avg	$0.56 \pm 0.10$	-	-	$0.18 \pm 0.10$	$0.18 \pm 0.062$
	Size	16	-	-	8	6
Cancer	Best	0.5	0.25	1.0	0.5	0.0
	Avg	$0.75 \pm 0.17$	-	-	$0.75 \pm 0.17$	$0 \pm 0$
	Size	8	-	-	8	1
Child	Best	0.5	0.0	1.0	0.37	0.41
	Avg	$0.54 \pm 0.04$	-	-	$0.45 \pm 0.04$	$0.52 \pm 0.020$
	Size	512	-	-	256	10
Climate	Best	0.0	0.0	1.0	0.0	0.14
	Avg	$0.0 \pm 0.0$	-	-	$0.0 \pm 0.0$	$0.32 \pm 0.09$
	Size	1	-	-	1	7
Covid 1	Best	0.0	0.0	1.0	0.0	0.0
	Avg	$0.0 \pm 0.0$	-	-	$0.0 \pm 0.0$	$0.0 \pm 0.0$
	Size	1	-	-	1	2
Covid 2	Best	0.33	0.0	1.0	0.33	0.0
	Avg	$0.33 \pm 0.0$	-	-	$0.33 \pm 0.0$	$0.22 \pm 0.15$
	Size	2	-	-	2	3
Covid 3	Best	0.6	0.0	1.0	0.0	0.2
	Avg	$0.85 \pm 0.16$	-	-	$0.1 \pm 0.1$	$0.43 \pm 0.13$
	Size	4	-	-	2	6
Covid 4	Best	1.0	1.0	1.0	1.0	0.0
	Avg	$1.0 \pm 0.0$	-	-	$1.0 \pm 0.0$	$0.0 \pm 0.0$
	Size	4	-	-	4	1
Genetic	Best	0.0	0.0	0.8	0.0	0.0
	Avg	$0.0 \pm 0.0$	-	-	$0.0 \pm 0.0$	$0.0 \pm 0.0$
	Size	2	-	-	2	4
MSU	Best	0.50	0.0	1.0	0.50	0.0
	Avg	$0.75 \pm 0.12$	-	-	$0.75 \pm 0.25$	$0.0 \pm 0.0$
	Size	8	-	-	4	1
Neighborhood	Best	0.75	0.0	1.0	1	0.16
	Avg	$0.87 \pm 0.12$	-	-	$1.0 \pm 0.0$	$0.5 \pm 0.15$
	Size	1	-	-	1	7
Opioids	Best	0.91	0.0	1.0	0.19	0.088
	Avg	$0.91 \pm 0.01$	-	-	$0.19 \pm 0.0$	$0.091 \pm 0.003$
	Size	2	-	-	1	2
Sachs	Best	0.64	0.0	1.0	0.11	0.11
	Avg	$0.69 \pm 0.04$	-	-	$0.17 \pm 0.04$	$0.21 \pm 0.044$
	Size	16	-	-	4	378
Supermarket	Best	0.75	0.75	1.0	0.66	0.16
	Avg	$0.79 \pm 0.04$	-	-	$0.66 \pm 0.0$	$0.33 \pm 0.13$
	Size	8	-	-	64	24

Table 4: Best result, mean and standard error of  $\hat{\mathcal{D}}_{top}$  across all graphs in the class obtained by each method (the lower the better) for data-driven methods. The size of the class obtained is reported for each method. Data are generated assuming linearity and uniform noise. Inconclusive experiments; i.e., results containing cycles or non terminating experiments, are regarded as having a maximum error, and are marked accordingly with  $\otimes$ .

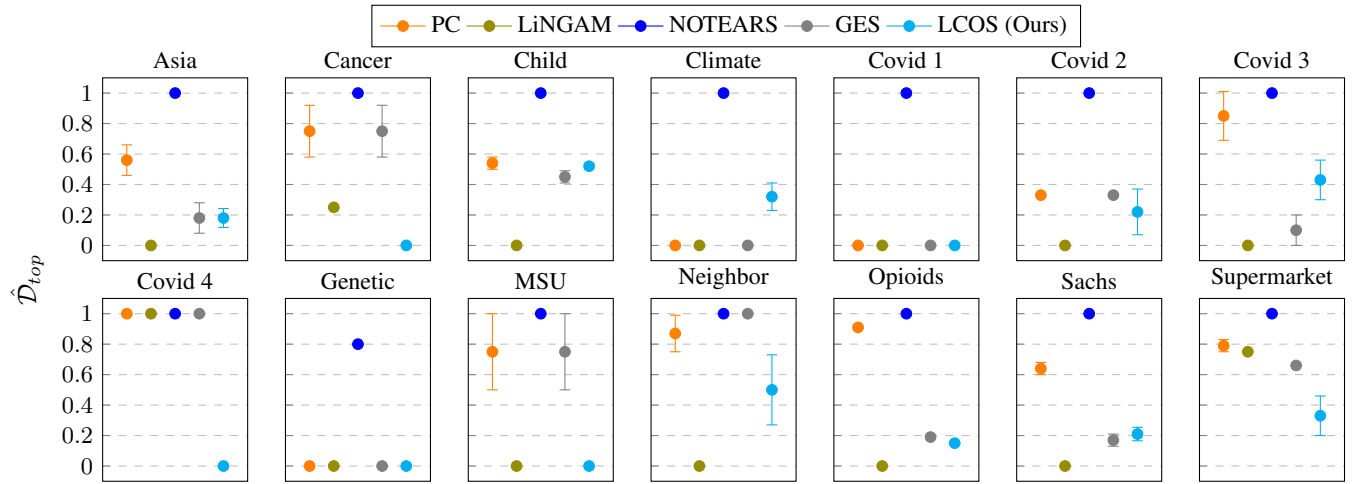


Figure 6: Mean and standard error of  $\hat{D}_{top}$  across all graphs in the class obtained by each method (the lower the better) for data-driven methods. Data are generated assuming linearity and uniform noise. Inconclusive experiments; i.e., results containing cycles or non terminating experiments, are regarded as having a maximum error, and are marked accordingly with  $\otimes$ .

<b>Dataset</b>	<b>Top. Error</b>	<b>gpt-4o-mini</b>	<b>llama3.1</b>	<b>mistral</b>
Asia	Min.	0.12	0.125	0.12
	Avg.	$0.18 \pm 0.062$	$0.125 \pm 0.0$	$0.26 \pm 0.9$
	Size	6	1	200
Cancer	Min.	0.0	0.0	0.0
	Avg.	$0 \pm 0$	$0.0 \pm 0.0$	$0.083 \pm 0.11$
	Size	1	1	3
Child	Min.	0.41	0.45	0.5
	Avg.	$0.52 \pm 0.020$	$0.45 \pm 0.0$	$0.5 \pm 0.0$
	Size	10	2	600
Climate	Min.	0.14	0.14	0.28
	Avg.	$0.32 \pm 0.09$	$0.23 \pm 0.06$	$0.28 \pm 0.0$
	Size	7	6	16
Covid 1	Min.	0.0	1.0	0.0
	Avg.	$0.0 \pm 0.0$	$1.0 \pm 0.0$	$0.25 \pm 0.25$
	Size	2	1	2
Covid 2	Min.	0.0	0.66	0.5
	Avg.	$0.22 \pm 0.15$	$0.66 \pm 0.0$	$0.5 \pm 0.0$
	Size	3	1	1
Covid 3	Min.	0.2	0.8	0.33
	Avg.	$0.43 \pm 0.13$	$0.8 \pm 0.0$	$0.33 \pm 0.0$
	Size	6	1	1
Covid 4	Min.	0.0	0.83	0.16
	Avg.	$0.0 \pm 0.0$	$0.83 \pm 0.0$	$0.16 \pm 0.0$
	Size	1	1	3
Genetic	Min.	0.0	0.8	0.25
	Avg.	$0.0 \pm 0.0$	$0.8 \pm 0.0$	$0.25 \pm 0.0$
	Size	4	4	6
MSU	Min.	0.0	0.0	0.16
	Avg.	$0.0 \pm 0.0$	$0.0 \pm 0.0$	$0.25 \pm 0.08$
	Size	1	1	2
Neighborhood	Min.	0.16	0.25	0.37
	Avg.	$0.5 \pm 0.15$	$0.25 \pm 0.0$	$0.42 \pm 0.061$
	Size	7	1	5
Opioids	Min.	0.088	⊗	⊗
	Avg.	$0.091 \pm 0.003$	-	-
	Size	2	-	-
Sachs	Min.	0.11	0.058	0.058
	Avg.	$0.21 \pm 0.044$	$0.24 \pm 0.04$	$0.078 \pm 0.027$
	Size	378	1	2
Supermarket	Min.	0.16	0.41	0.33
	Avg.	$0.33 \pm 0.13$	$0.41 \pm 0.0$	$0.33 \pm 0.0$
	Size	24	1	2

Table 5: Best result, mean and standard error of  $\hat{\mathcal{D}}_{top}$  across all graphs in the class obtained by each method (the lower the better) using different LLMs (gpt-4o-mini, llama3.1, mistral). The size of the class obtained is reported for each method. Inconclusive experiments; i.e., results containing cycles or non terminating experiments, are regarded as having a maximum error, and are marked accordingly with  $\otimes$ .